Morphological Control of Helical Structures of an ABC-Type Triblock Terpolymer by Distribution Control of a Blending Homopolymer in a Block Copolymer Microdomain

ARTICLE *in* MACROMOLECULES · AUGUST 2013

Impact Factor: 5.8 · DOI: 10.1021/ma401193u

9 AUTHORS, INCLUDING:

Takeshi Higuchi
Tohoku University
50 PUBLICATIONS **915** CITATIONS
SEE PROFILE

Song Hong
Beijing University of Chemical Technology
31 PUBLICATIONS **308** CITATIONS
SEE PROFILE

Atsushi Takahara
Kyushu University
487 PUBLICATIONS **8,480** CITATIONS
SEE PROFILE

Hiroshi Jinnai
Tohoku University
234 PUBLICATIONS **4,233** CITATIONS
SEE PROFILE

Macromolecules

Article

pubs.acs.org/Macromolecules

Morphological Control of Helical Structures of an ABC-Type Triblock Terpolymer by Distribution Control of a Blending Homopolymer in a Block Copolymer Microdomain

Takeshi Higuchi,[†,‡] Hidekazu Sugimori,[§,&] Xi Jiang,[‡] Song Hong,[‡] Kazuyuki Matsunaga,[§,$] Takeshi Kaneko,[§,%] Volker Abetz,[∥,⊥] Atsushi Takahara,[†,‡,#] and Hiroshi Jinnai*[,†,‡,#]

[†]Takahara Soft Interfaces Project, Exploratory Research for Advanced Technology (ERATO), Japan Science and Technology Agency (JST), 744 Motooka, Nishi-ku, Fukuoka 819-0395, Japan

[‡]Institute for Materials Chemistry and Engineering (IMCE), Kyushu University, 744 Motooka, Nishi-ku, Fukuoka 819-0395, Japan

[§]Department of Macromolecular Science and Engineering, Graduate School of Science and Engineering, Kyoto Institute of Technology, Matsugasaki, Sakyo-ku, Kyoto 606-8585, Japan

[∥]Institute of Physical Chemistry, University of Hamburg, Grindelallee 117, 20146 Hamburg, Germany

[⊥]Institute of Polymer Research, Helmholtz-Zentrum Geesthacht, Max-Planck-Str. 1, 21502 Geesthacht, Germany

[#]International Institute for Carbon-Neutral Energy Research (WPI-I2CNER), Kyushu University, 744 Motooka, Nishi-ku, Fukuoka 819-0395, Japan

Supporting Information

ABSTRACT: The control of microphase-separated structures in a poly(styrene-*block*-butadiene-*block*-methyl methacrylate) (SBM) was investigated in three dimensions by transmission electron microtomography. Neat SBM self-assembled into a double-helical structure of polybutadiene (PB) domains around hexagonally packed core polystyrene (PS) cylinders in a poly(methyl methacrylate) matrix. When PS homopolymer with a lower molecular weight than that of the PS block in SBM was added to the SBM, the PB domains transformed from double-helical structures to spherical domains, while maintaining the helical trajectories. In contrast, adding a higher molecular weight PS to the SBM changed the helical structures from double- to triple-stranded structures and even to four-stranded structures. The helical structures of the PB domains were strongly affected by the distribution of the blended polystyrenes in the core cylindrical PS domains.

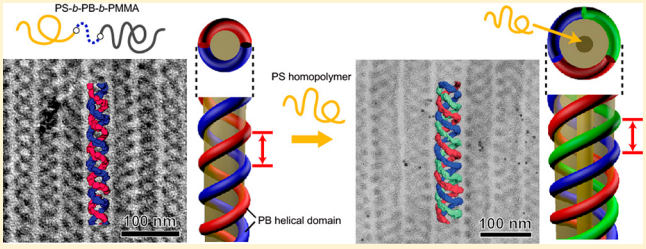

1. INTRODUCTION

Block copolymers, consisting of covalently bonded chemically dissimilar sequences, exhibit highly periodic microphase-separated structures. The characteristic lengths of the structures are determined by the molecular size and are in the 10−100 nm range. The simplest block copolymers are linear AB-type diblock copolymers. The volume fractions and Flory−Huggins interaction parameters, χ, of each component (χ_{AB}) of the blocks determine the morphologies observed. Morphologies include body-centered cubic arrays of spheres, hexagonally packed cylinders, bicontinuous gyroids, and alternating lamellae.[1] Three-component systems, such as ABC-type linear triblock terpolymers, form much more complex and intriguing microphase-separated structures compared with AB-type diblock copolymers.[2]

With the rapid progress of nanotechnology, periodic nanostructures of triblock terpolymers have been used for many applications, including templates for nanopatterning, electrolyte films, low-*k* films, and nanoporous membranes.[3−9] An intriguing double-helical morphology has been reported in an ABC-type triblock terpolymer.[10−12] Ho et al. also discovered a left-handed helical structure in the bulk material of a diblock copolymer.[13] The chiral entity of the constituent blocks plays an important role in forming their helical superstructures. Because these helical morphologies have great potential for a wide variety of applications such as electromagnetic wave absorber, metamaterials, etc., by converting helical structures to conductive domains, the control of helical handedness, pitch, diameter, and number of helical strands is an important challenge.

The morphology of microphase-separated structures can be controlled by changing the relative volume fraction of each component with respect to the other component blocks. However, this method involves the synthesis of ABC-type terpolymers. The simplest nonsynthetic way to change the relative volume fraction is to add to the blend a homopolymer

Received: June 11, 2013
Revised: August 12, 2013
Published: August 26, 2013

of the same kind as one of the constituent blocks. Hashimoto et al. reported that when an A-homopolymer is mixed with AB-diblock copolymers, the distribution of the A-homopolymer in the A-microdomain of the AB-diblock copolymer is closely related to the ratio of the A-homopolymer to the A-block. This ratio, r_s, is defined as $r_s = N_{A,homo}/N_{A,block}$, where $N_{A,homo}$ and $N_{A,block}$ are the degrees of polymerization of the A-homopolymer and A-block chain, respectively.[14,15] If $r_s \ll 1$ (wet brush regime), the A-homopolymer uniformly swells the A-microdomain, whereas when $r_s \approx 1$ or $r_s \gg 1$ (dry brush regime), the A-homopolymer is localized in the center of the A-microdomain. These different homopolymer distributions inside the A microdomain strongly affect the block copolymer morphologies.

Although a number of studies on ABC-type terpolymers have been carried out in order to understand their morphological behaviors, methods for precise morphological control remain relatively undeveloped. One of the main difficulties in achieving control in terpolymers is the complexity of their morphology. The morphologies are often too complicated to characterize by conventional experimental techniques, such as transmission electron microscopy (TEM) and small-angle X-ray and neutron scattering. Transmission electron microtomography (electron tomography; ET)[16] is among the most powerful microscopic techniques because it can provide three-dimensional (3D) images of the microphase-separated structures.[17−21] The technique has been used to study various aspects of microphase-separated diblock copolymer structures, including the chain conformation in microdomain morphologies,[22,23] grain boundary morphologies,[24] self-assembly processes,[25] and the stability of microphase-separated structures.[26]

ET has also been used to characterize the complicated morphology of ABC triblock terpolymers.[27,28] Previously, we have reported that a linear ABC-type triblock terpolymer—composed of polystyrene, polybutadiene, and poly(methyl methacrylate) blocks—forms double-helical structures.[29,30] In the present study, we have demonstrated that the helical morphology can be controlled by adding homopolystyrene (hPS) of two different molecular weights and homopolybutadiene (hPB).

2. EXPERIMENTAL SECTION

2-1. Materials. A poly(styrene-*block*-butadiene-*block*-methyl methacrylate) (SBM) triblock terpolymer was synthesized by the sequential anionic polymerization of styrene, butadiene, and methyl methacrylate in tetrahydrofuran (THF) in the presence of lithium alkoxides, with *sec*-butyllithium as the initiator. hPS of two different molecular weights, hPS_{84} and hPS_{970}, was used. The number-average molecular weight (M_n) of hPS_{84} was 8.4×10^3 and that of hPS_{970} was 9.7×10^4, which were lower and higher than that of the PS block of the SBM triblock terpolymer, respectively. The ratio of the degree of polymerization of hPS (N_{hPS}) to the S block chain of SBM (N_{PS}) is defined as $r_s = N_{hPS}/N_{PS}$. The r_s values of hPS_{84} and hPS_{970} were 0.25 and 2.9, respectively. hPB with a lower molecular weight than that of the PB block in SBM was also used. For hPB, M_n was 4.0×10^3 and r_s was 0.34. The molecular characteristics of the polymers are summarized in Table 1.

2-2. Specimens. Blends of SBM and hPS (SBM/hPS) with various compositions were prepared as shown in Table 2. The film specimens were prepared by casting solutions of ∼5 wt % of the SBM triblock terpolymer or SBM/hPS in chloroform ($CHCl_3$) at room temperature. The cast films were then annealed at 100 °C for 24 h, followed by heating at 170 °C under vacuum for a further 24 h. The annealed films were ultramicrotomed to a thickness of ∼150 nm using an Ultracut UCT microtome (Leica, Germany) with a diamond knife at room temperature. The ultrathin section was transferred onto a Cu mesh grid with a polyvinyl formal supporting membrane. The ultrathin section was stained with osmium tetroxide (OsO_4) vapor for 1 h. Prior to the electron microscopy experiments, gold particles 5 nm in diameter were placed on the ultrathin section from colloidal aqueous solution. Blends of SBM, hPS, and hPB (SBM/hPS/hPB) were also prepared as shown in Table 3. The same protocol was used to prepare SBM/hPS/hPB.

Table 1. Molecular Characteristics of SBM Triblock Terpolymer, Homopolystyrenes, and Homopolybutadiene

	M_n (kg mol^{-1})	M_w/M_n	S/B/M (volume fractions)
SBM	34/11.9/124.1	1.03	0.21/0.09/0.70
hPS_{84}	8.4/−/−	1.03	1.0/−/−
hPS_{970}	97/−/−	1.01	1.0/−/−
hPB	−/4.0/−	1.10	−/1.0/−

Table 2. SBM and hPS Blend Compositions

sample no.	composites	weight fractions (SBM/hPS)	total volume fraction of PS in SBM/hPS (Φ_{PS})
0	neat SBM	1.00/0	0.21
1	SBM/hPS_{84}	0.97/0.03	0.24
2	SBM/hPS_{84}	0.94/0.06	0.26
3	SBM/hPS_{84}	0.90/0.10	0.30
4	SBM/hPS_{84}	0.88/0.12	0.32
5	SBM/hPS_{84}	0.81/0.19	0.37
6	SBM/hPS_{970}	0.98/0.02	0.23
7	SBM/hPS_{970}	0.97/0.03	0.24
8	SBM/hPS_{970}	0.96/0.04	0.25
9	SBM/hPS_{970}	0.94/0.06	0.26
10	SBM/hPS_{970}	0.90/0.10	0.30
11	SBM/hPS_{970}	0.88/0.12	0.32
12	SBM/hPS_{970}	0.81/0.19	0.37

Table 3. SBM, hPS, and hPB Blend Compositions

sample no.	composites	weight fractions (SBM/hPS/hPB)	volume fraction of PS (Φ_{PS})
13	SBM/hPS_{84}	1/0.2/0	0.350
14	SBM/hPS_{84}/hPB	1/0.2/0.01	0.345
15	SBM/hPS_{84}/hPB	1/0.2/0.03	0.338

2-3. TEM and ET Observations. We conduced 3D observations by TEM and ET using a JEM-2200FS microscope (JEOL, Ltd., Japan) operated at 200 kV and equipped with a slow-scan USC 4000 CCD camera (Gatan, Inc.). A series of TEM images were acquired at tilt angles in the range of ±75° at an angular interval of 1°. The tilt series of the TEM images were then aligned by the fiducial marker method, using gold nanoparticles as the fiducial markers.[31] The tilt series of TEM images after the alignment were reconstructed by filtered back-projection.[32]

3. RESULTS AND DISCUSSION

3-1. Morphological Characterization of SBM/hPS_{84} and SBM/hPS_{970} Films. The SBM triblock terpolymer was blended with hPS of two different molecular weights in order to control the morphology. We have previously reported that neat SBM adopts a 3D morphology where the PB domains form a double-helical structure around hexagonally packed PS cylinders in a PMMA matrix. The ET observations of the double-helical structure revealed that the diameter (D) of the PS core cylinder was 24 ± 0.87 nm and the pitch of the PB helices was 53 ± 1.63 nm. When the lower molecular weight hPS_{84} homopolymer was blended with SBM, the PB domains underwent a morphological transition (Figure S-1). When the

dx.doi.org/10.1021/ma401193u | Macromolecules 2013, 46, 6991−6997

total volume fraction of PS in the system (Φ_{PS}) reached 0.32, the double-helical structures became partially disconnected. As Φ_{PS} increased further to 0.37, the PB domains transformed completely into spherical domains around the core PS cylinder and maintained the helical trajectories.[29]

In the present study, a small amount of hPS_{970}, which has a higher molecular weight than that of hPS_{84}, was blended into SBM. Figures 1a–c show TEM images of SBM/hPS_{970} with

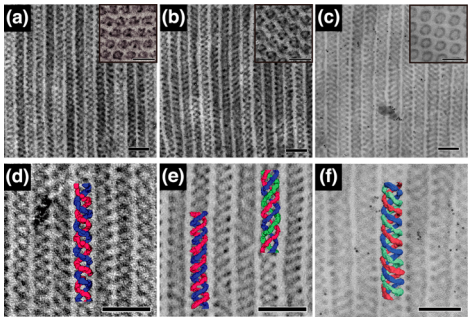

Figure 1. TEM images of SBM/hPS_{970}. (a) Φ_{PS} = 0.23, (b) 0.24, and (c) 0.26. Insets in (a–c) are images from the vertical to the hexagonally packed PS cylinders. Reconstructed 3D images of SBM/hPS_{970} obtained by ET are overlaid on the corresponding regions in the TEM images of (d) Φ_{PS} = 0.23, (e) 0.24, and (f) 0.26. PB microdomains are blue, red, and green in the 3D images. Scale bars represent 100 nm.

Φ_{PS} = 0.23, 0.24, and 0.26 (neat SBM: Φ_{PS} = 0.21). The dark regions correspond to the PB microdomains that were stained with OsO_4. These figures show the striped pattern of the PB microdomains, which are similar to the images of neat SBM. The PS core cylinders were hexagonally packed in the PMMA matrix (insets in Figures 1a–c). In the case of Φ_{PS} = 0.26, most of the PB domains formed ordered microphase-separated structures; however, a narrow disordered region was also visible (Figure S-2a). When the blend ratio exceeded Φ_{PS} = 0.30, macrophase separation between the terpolymer and the added hPS occurred (Figure S-2b).

To determine the 3D structures of the PB domains, the SBM/hPS_{970} films with Φ_{PS} = 0.23, 0.24, and 0.26 were observed by ET. The 3D structures of the PB domains were overlaid on the corresponding TEM images at a tilt angle of 0° (Figure 1d–f). Figure 1d shows the double-helical structures were formed at Φ_{PS} = 0.23. In the case of Φ_{PS} = 0.24, most of the PB domains formed double-helical structures, although a small number of triple-helical structures were visible (Figure 1e). As the amount of hPS_{970} increased, the fraction of triple-helical structures increased until Φ_{PS} = 0.26 (Figure 1f). It is intriguing that a small number of four-stranded helical structures were observed at Φ_{PS} = 0.26. The morphologies of the SBM/hPS_{970} films are summarized in Table 4.

3-2. Structural Analysis of SBM/hPS_{84} and SBM/hPS_{970} Films. Figure 2a shows the diameter of the PS core cylinder (D) as a function of Φ_{PS}. The squares, circles, and triangles show D for neat SBM, SBM/hPS_{84}, and SBM/hPS_{970}, respectively. At total PS compositions higher than 0.24, SBM/hPS_{970} had two distinct diameters at the same Φ_{PS}. For example, at Φ_{PS} = 0.24, there were two values of D, which corresponded to the double- and triple-helical structures, respectively. The numbers next to the points plotted on the graph indicate the number of PB helical structures around the PS core cylinder. The color of the filled triangle shows the

Table 4. Fractions of Microstructures in SBM/hPS_{970}

	fraction of the microstructures				
Φ_{PS}[a]	double helix	triple helix	four-stranded helix	disordered microdomain	macrodomain
0.21 (neat SBM)	1.0				
0.23	1.0				
0.24	0.8	0.2			
0.25	0.16	0.84			
0.26		0.83	0.04	0.13	
0.30			(0.08)[b]	0.87	0.05
0.32				0.95	0.05
0.37				0.82	0.18

[a]The measured area in each Φ_{PS} was about 130 μm^2. [b]The total fraction of the helical morphologies is 0.08 when Φ_{PS} = 0.30.

probability of the corresponding morphology; the structures with black symbols are more probable than those with gray symbols. For SBM/hPS_{84}, D increased almost linearly with Φ_{PS}. In contrast, although D for the double-helical structures for SBM/hPS_{970} increased proportionally with Φ_{PS} similar to SBM/hPS_{84}, D for the triple- and four-stranded helical structures increased more rapidly than that for the double-helical structure. The values of D for the triple- and four-stranded helical structures were 1.5- and 2-fold greater than that of neat SBM, respectively, as indicated by the arrow in Figure 2a.

The distribution of the A-homopolymer in the microphase-separated structure is closed related to the ratio of the degree of polymerization of the homopolymer and the block chains (r_s) when the A-homopolymer is added to the A–B diblock copolymer.[14,15] In the wet brush regime ($r_s \ll 1$), the A-homopolymer is distributed uniformly in the A-microdomain and thus swells only the A-domain of the A-B diblock copolymer. However, in the dry brush regime ($r_s \approx 1$ or $r_s \gg 1$), the A-homopolymer tends to be localized at the center of the A-microdomain. On the basis of these established models, we constructed two models in which the distribution of hPS inside the PS core cylinder was assumed depending on r_s (Figure 2b,c). The hPS_{84} homopolymer was shorter than the SBM PS block in SBM/hPS_{84}, where r_s = 0.25. Therefore, this homopolymer was expected to uniformly swell the PS core cylinders (Figure 2b). In this case, the diameter in SBM/hPS_{84} (D_{84}) as a function of Φ_{PS} can be described as

$$D_{84} = \sqrt{\frac{\phi_{PS}(1-\phi_{PS0})}{\phi_{PS0}(1-\phi_{PS})}} D_0 \quad (1)$$

Here, D_0 and Φ_{PS0} are the diameter and the volume fraction of PS in neat SBM, respectively. Winey et al. reported that, even though A-homopolymer with lower molecular weight than that of A-block in A–B block copolymer, the A-homopolymers did not distributed uniformly in the lamellar A-domains above a certain A-homopolymer concentration.[33,34] In our experiments, the concentration of A-homopolymer was lower than such A-homopolymer concentration where the transition from nonuniform to uniform distribution of A-homopolymer occurs.

The hPS_{970} homopolymer was longer than the SBM PS block in SBM/hPS_{970}, where r_s = 2.9. Thus, hPS_{970} should be localized in the center of the PS core cylinder (Figure 2c). It was assumed that the localized hPS_{970} molecules adopted a Gaussian chain conformation, which is the state where the

dx.doi.org/10.1021/ma401193u | Macromolecules 2013, 46, 6991–6997

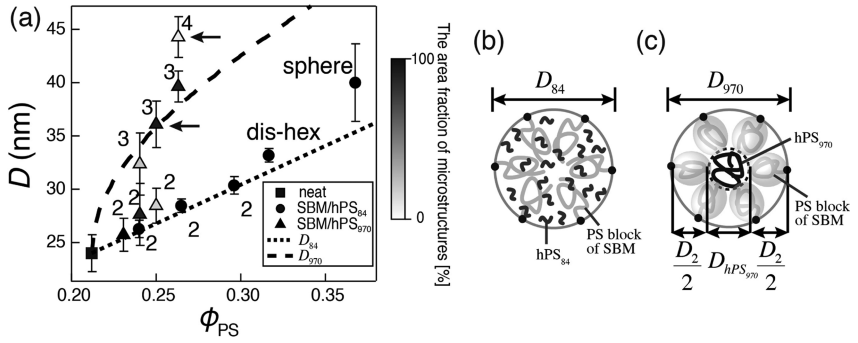

Figure 2. (a) Diameter of the PS cylinder (D) of SBM/hPS$_{84}$ and SBM/hPS$_{970}$ as a function of the volume fraction of PS (Φ_{PS}). Shading of the markers corresponds to the area fraction of the microdomains. Dotted and dashed lines indicate D calculated from the models shown in (b) and (c). Models of the distribution of (b) hPS$_{84}$ and (c) hPS$_{970}$ in the PS cylinders in SBM. hPS block chains are shown in black, and PS block chains are shown in gray.

molecules are unperturbed by the surrounding PS block chains. It was also assumed that hPS$_{970}$ did not affect the chain conformation of the PS block chains. Therefore, the diameter of SBM/hPS$_{970}$ (D_{970}) as a function of Φ_{PS} can be described as a simple sum of the diameters of the PS cylinders formed independently at each SBM/hPS$_{970}$ composition

$$D_{970} = D_0 + D_{hPS} = \left(1 + \sqrt{\frac{\phi_{PS} - \phi_{PS0}}{\phi_{PS0}(1 - \phi_{PS})}}\right) D_0 \quad (2)$$

Here, D_{hPS} is the diameter of the PS cylinder formed by hPS$_{970}$.

D_{84} and D_{970} calculated with eqs 1 and 2 are plotted in Figure 2a as a dotted and a dashed line, respectively. D_{84} agrees well with the experimental results for SBM/hPS$_{84}$ for $\Phi_{PS} < 0.32$, suggesting that hPS$_{84}$ swells the whole PS core cylinder. SBM/hPS$_{970}$ also follows the dotted line (D_{84}) for $\Phi_{PS} < 0.23$. Thus, the long hPS$_{970}$ homopolymer does not localize in the center of the core cylinder when the amount of hPS is small. The observed diameter of the triple-helical structure agreed with D_{970}, implying that the number of helical domains changed from 2 to 3 as hPS$_{970}$ began localizing at the center.

3-3. Morphological Transition Mechanism in SBM/hPS$_{84}$ and SBM/hPS$_{970}$. To clarify the mechanism of the morphological transition from the double-helical structure to spherical domains in SBM/hPS$_{84}$, the length (L), diameter (s), and volume (V_{PB}) of the PB helical structures per pitch (p) were measured from the 3D images ($\Phi_{PS} < 0.32$). L was calculated from $L = (p^2 + (\pi D)^2)^{1/2}$. As previously reported,[28] the pitch decreased as Φ_{PS} increased. L increased from 92 nm in neat SBM to 103 nm (Figure 3a). In contrast, s decreased from 10.2 nm in neat SBM to 9.78 nm (Figure 3b). In this Φ_{PS} region, V remained constant at 7500 nm^3, indicating that the number of the SBM molecules per pitch did not depend on D. Thus, the PB block chains inside the PB microdomains stretched as Φ_{PS} increased. The elongation of the PB helical domains would reduce the conformational entropy of the PB block chains. In order to mitigate the conformational entropy loss, the PB helical domains began to separate, which induced the transformation of the helical domains to spherical domains when Φ_{PS} is higher than 0.350 (Figures S-1d and S-3a).

Figures 4a and 4b show the pitch and length of the PB helical structures measured from the 3D structures of SBM/hPS$_{84}$ and SBM/hPS$_{970}$. The pitch and length of the triple-helical structures were approximately 1.5-fold larger than those of the double-helical structures formed in neat SBM, indicated by the arrows in Figure 4. In the four-stranded helical structures,

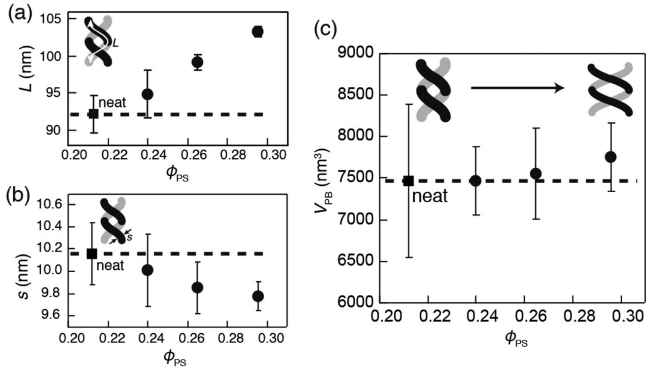

Figure 3. (a) Diameter s, (b) contour length L, and (c) volume V_{PB} of PB microdomains as a function of the volume fraction of PS (Φ_{PS}) in SBM/hPS$_{84}$. Dashed lines in each plot indicate s, L, and V_{PB} of neat SBM.

the pitch and length were 2-fold larger. As described in section 3-2, the diameters of the triple- and four-stranded helical structures were 1.5- and 2-fold larger than that of neat SBM.

Let us next consider the meaning of the 1.5- and 2-fold increases in D, p, and L for the triple- and four-stranded helical structures. The double-helical structure with diameter, D_2, and pitch, p_2, can be simplified by cutting and unwrapping the 3D structure (Figure 5b) onto a 2D plane (Figure 5c). A triangle composed of three edges with lengths of p_2, πD_2, and L_2 is now the simplest structural element of the double-helical structure (Figure 5d). Based on the results in Figures 2 and 5, the diameter (D_3) and the PB length (L_3) per pitch (p_3) of the triple-helical structure were 1.5-fold larger than the values for the double-helical structure. The structural elements for the triple-helical structure of SBM/hPS$_{970}$ are shown in Figure 5e. The triangles for the double- and triple-helical structures are homothetic; the angles between the two sides in the triangles (α) are identical in the two structures, $\alpha_2 = \alpha_3$. Here, α_2 and α_3 are the angles of the double-helical structure in neat SBM and that of the triple-helical structure in SBM/hPS$_{970}$ = 0.96/0.04, respectively (Φ_{PS} = 0.25, the filled triangle indicated by the arrow in Figure 4a). Additionally, the homothetic relationship is also observed in the four-stranded helical structure because p_4, πD_4, and L_4 are 2-fold larger than those of the double-helical structure.

The meaning of α in terms of the block chain conformation in the helical structures must be considered. Because it is difficult to visualize the conformation of the polymer chains by

dx.doi.org/10.1021/ma401193u | Macromolecules 2013, 46, 6991−6997

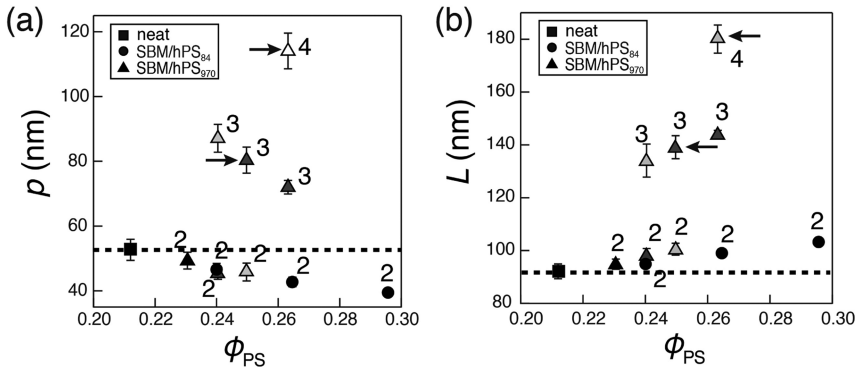

Figure 4. (a) Helical pitch (p) and (b) length (L) of the PB microdomain as a function of the volume fraction of PS (Φ_{PS}) in SBM/hPS$_{84}$ and SBM/hPS$_{970}$. Shading of the markers corresponds to the area fraction of the microdomains. Dashed lines indicate p and L in neat SBM.

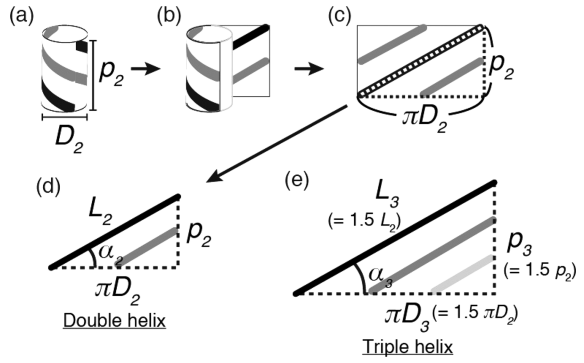

Figure 5. Simplification of the helical structures of the PB domains from a 3D structure to a 2D plane. (a) Simplified double-helical structure with one helical pitch. (b) Double-helical structure unwrapped from the PS cylinder. (c) Unwrapped double-helical structure on a 2D plane. (d) Single helix of the double-helical structure with one helical pitch is extracted as a right triangle composed of three edges, p_2, πD_2, and L_2. (e) Right triangle for the triple-helical structure. Each edge (p_3, πD_3, and L_3) is 1.5-fold larger than those of the double-helical structure. Triangles for the double- and triple-helical structures have a homothetic relationship (see demonstration movie in the Supporting Information).

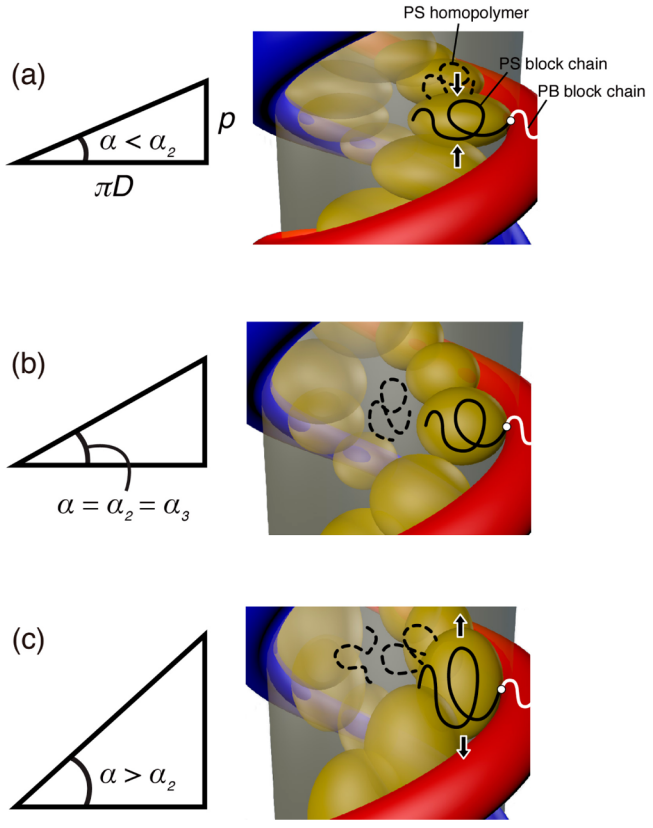

Figure 6. Schematics of the chain distributions of the terpolymer and homopolymer inside the PS core cylinder with different helical angles. (a) $\alpha < \alpha_2$, (b) $\alpha = \alpha_2 = \alpha_3$, and (c) $\alpha > \alpha_2$.

TEM and ET, it is inferred from the shape and arrangement of the microdomains. The PB domains were helically arranged around the core PS cylindrical domain; therefore, the SBM PS block chains must also be arranged in a helix inside the PS core cylinder because of the connectivity between the PS and PB blocks. Therefore, the helical pitch should be influenced by the conformation of the PS block chains. Figure 2 shows the diameter of the core PS cylinder as a function of the total volume fraction. The diameter of the triple-helical structure, D_3, lies exactly on the dashed line in Figure 2a, indicating that the hPS chains are located in the center of the core PS cylinder (Figure 2c). Therefore, hPS$_{970}$ does not interact strongly with the PS block chains of the SBM terpolymer. If this is the case, the helically arranged PS block chains should also be present in the PS core cylinder (Figure 6b). In contrast, if hPS$_{970}$ interacts with the PS block chains, the chain conformation of the PS block chains would change and the distance between the PS block chains along the cylindrical axis would also change, thus altering the helical pitch (Figure 6a,c). If hPS$_{970}$ does not interact with the PS, the angle, α, should be the same as the angle of the helical structure in neat SBM (without blending), $\alpha = \alpha_2 = \alpha_3$, whereas if it does, $\alpha_2 \neq \alpha_3$.

Figure 7 summarizes the chain distributions of the SBM terpolymer and the PS homopolymer inside the PS core cylinder. Figure 7a illustrates the double-helical structure of neat SBM terpolymer. As hPS$_{970}$ was added to SBM up to Φ_{PS} = 0.24, D increased and p decreased as it did for the wet brush regime in SBM/hPS$_{84}$ (Figures 2 and 4). This is because the added hPS$_{970}$ behaved as it would for the wet brush regime and swelled the entire PS core cylinder (Figure 7b). As the homopolymer was added, hPS$_{970}$ began to localize at the center of the core PS cylinder for $\Phi_{PS} > 0.24$, and the PS block chains and hPS$_{970}$ stopped interacting with each other. The number of the helical microdomains simultaneously changed from 2 to 3. This process may be beneficial in terms of the free energy because the PS block chains can return to the original

dx.doi.org/10.1021/ma401193u | Macromolecules 2013, 46, 6991−6997

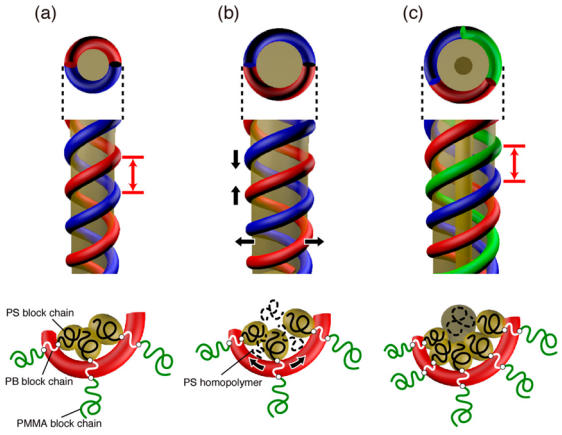

Figure 7. Schematic illustration of chain distributions of terpolymer and homopolymer inside the PS core cylinder of the double- and triple-helical structures in SBM/hPS$_{970}$. (a) Double-helical structure of neat SBM. (b) After the addition of a small amount of hPS$_{970}$, hPS$_{970}$ is uniformly blended into the entire PS core cylinder. The diameter of the PS cylinder increases, and the pitch of the PB helical domain decreases. (c) hPS$_{970}$ is located at the center of the core PS cylinder.

conformation in neat SBM. This relaxation of the chain conformation of the PS blocks was deduced from the following experimental results: the angle, α, of the structural element is the same (Figure 5b), and the distance between the neighboring helical domains (indicated by red arrows in Figure 7a,c) is exactly the same for neat and blended SBM.

4. SUMMARY

In this study, we controlled the helical morphology of the linear ABC-triblock terpolymer, SBM, by controlling the distribution of the blended homopolymers. The homopolymers were hPS of two different molecular weights, which produced wet and dry brush systems, and hPB. ET structural analysis was conducted to determine the 3D morphologies and quantitative structural parameters, such as the diameter, length, and volume of the helical domains, in order to clarify the blend mechanisms. When hPS with a lower molecular weight than the SBM PS block was added, the PB domains changed from double-helical structures to spherical domains along the helical trajectories. In contrast, when hPS with a higher molecular weight than the SBM PS block was added, the helical structure changed from a double to a triple- or four-stranded structure. ET showed that the low weight hPS uniformly swelled in the SBM PS cylinders, which induced the elongation of the SBM PB block chains as the hPS blend ratio increased. The elongation may cause a conformational energy loss in the PB block chains. The lessening of the energy loss could be the driving force of the transition from the double-helical to the spherical PB domains. Moreover, the addition of hPB caused the reappearance of the double-helical structures, even though the helical domain was elongated by hPS (Figure S-3). This suggests that the hPB molecules were localized in the PB domains formed by the SBM PB chains and allowed the spheres to reconnect to each other. However, when a small amount of high weight hPS was added, the hPS molecules blended into the SBM PS block chain, as it did for the low weight hPS. This swelled the PS core cylinder, which induced conformational energy loss in the PB block chains. The amount of hPS that can blend into the SBM PS block chain is limited. When the blending ratio exceeds the limit, the hPS molecules start to localize in the center of the PS cylinder. The morphological transition from the double- to triple-helical structure occurred to mitigate the conformational energy loss of the block chains because the chain conformations of the double- and triple-helical structures are similar.

■ ASSOCIATED CONTENT

Supporting Information

TEM images of SBM/hPS$_{84}$; TEM images of SBM/hPS$_{970}$ for Φ_{PS} = 0.26 and 0.32; the morphological transition in SBM/hPS$_{970}$/hPB; and a demonstration movie showing the homothetic relationship between the double- and triple-helical structures. This material is available free of charge via the Internet at http://pubs.acs.org.

■ AUTHOR INFORMATION

Corresponding Author

*E-mail: hjinnai@cstf.kyushu-u.ac.jp.

Present Addresses

[&]H.S.: KRI Inc., Kyoto Research Park, 134, Chudoji Minami-machi, Shimogyo-ku, Kyoto 600-8813, Japan.

[$]K.M.: Sumitomo Chemical Co., Ltd., 2-1, Kitasode, Sodegaura City, Chiba 299-0295, Japan.

[%]T.K.: JEOL Ltd., 1-2, Musashino 3-chome Akishima Tokyo 196-8558, Japan.

Notes

The authors declare no competing financial interest.

■ ACKNOWLEDGMENTS

The authors are grateful to Dr. H. Morita of National Institute of Advanced Industrial Science and Technology for his valuable discussions and comments. This work was supported by Grants-in-Aid No. 24310092 and 25706006 from the Ministry of Education, Culture, Sports, Science, and Technology.

■ REFERENCES

(1) Bates, F. S.; Fredrickson, G. H. *Phys. Today* **1999**, *52*, 32−38.
(2) Abetz, V.; Goldacker, T. *Macromol. Rapid Commun.* **2000**, *21*, 16−34.
(3) Guarini, K. W.; Black, C. T.; Zhang, Y.; Kim, H.; Sikorski, E. M.; Babich, I. V. *J. Vac. Sci. Technol., B* **2002**, *20*, 2788−2792.
(4) Hamley, I. W. *Nanotechnology* **2003**, *14*, R39−R54.
(5) Stoykovich, M. P.; Muller, M.; Kim, S.; Solak, H. H.; Edwards, E. W.; Pablo, J. J.; Nealey, P. F. *Science* **2005**, *308*, 1442−1446.
(6) Widawski, G.; Rawiso, M.; Francois, B. *Nature* **1994**, *369*, 387−389.
(7) Freer, E. M.; Krupp, L. E.; Hinsberg, W. D.; Rice, P. M.; Hedrick, J. L.; Cha, J. N.; Miller, R. D.; Kim, H. *Nano Lett.* **2005**, *5*, 2014−2018.
(8) Peinemann, K.; Abetz, V.; Simon, P. W. *Nat. Mater.* **2007**, *6*, 992−996.
(9) Ro, H. W.; Peng, H.; Niihara, K. I.; Lee, H. J.; Lin, E. K.; Karim, A.; Gidley, D. W.; Jinnai, H.; Yoon, D. Y.; Soles, C. L. *Adv. Mater.* **2008**, *20*, 1934−1939.
(10) Krappe, U.; Stadler, R.; Voigtmartin, I. *Macromolecules* **1995**, *28*, 4558−4561.
(11) Breiner, U.; Krappe, U.; Abetz, V.; Stadler, R. *Macromol. Chem. Phys.* **1997**, *198*, 1051−1083.
(12) Schacher, F.; Yuan, J. Y.; Schoberth, H. G.; Muller, A. H. E. *Polymer* **2010**, *51*, 2021−2032.
(13) Tseng, W. H.; Chen, C. K.; Chiang, Y. W.; Ho, R. M.; Akasaka, S.; Hasegawa, H. *J. Am. Chem. Soc.* **2009**, *131*, 1356−1357.
(14) Hashimoto, T.; Tanaka, H.; Hasegawa, H. *Macromolecules* **1990**, *23*, 4378−4386.
(15) Koizumi, S.; Hasegawa, H.; Hashimoto, T. *Macromolecules* **1994**, *27*, 6532−6540.

(16) Frank, J. In *Principles of Electron Tomography*; Frank, J., Ed.; Plenum Press: New York, 1992.
(17) Kawase, N.; Kato, M.; Nishioka, H.; Jinnai, H. *Ultramicroscopy* **2007**, *107*, 8−15.
(18) Jinnai, H.; Nishikawa, Y.; Ikehara, T.; Nishi, T. *Adv. Polym. Sci.* **2004**, *170*, 115−167.
(19) Higuchi, T.; Motoyoshi, K.; Sugimori, H.; Jinnai, H.; Yabu, H.; Shimomura, M. *Soft Matter* **2012**, *8*, 3791−3797.
(20) Jinnai, H.; Spontak, R. J.; Nishi, T. *Macromolecules* **2010**, *43*, 1675−1688.
(21) Sugimori, H.; Nishi, T.; Jinnai, H. *Macromolecules* **2005**, *38*, 10226−10233.
(22) Jinnai, H.; Nishikawa, Y.; Spontak, R. J.; Smith, S. D.; Agard, D. A.; Hashimoto, T. *Phys. Rev. Lett.* **2000**, *84*, 518−521.
(23) Morita, H.; Kawakatsu, T.; Doi, M.; Nishi, T.; Jinnai, H. *Macromoledules* **2008**, *41*, 4845−4849.
(24) Jinnai, H.; Sawa, K.; Nishi, T. *Macromolecules* **2006**, *39*, 5815−5819.
(25) Niihara, K.; Sugimori, H.; Matsuwaki, U.; Hirato, F.; Morita, H.; Doi, M.; Masunaga, H.; Sasaki, S.; Jinnai, H. *Macromolecules* **2008**, *41*, 9318−9325.
(26) Niihara, K.; Matsuwaki, U.; Torikai, N.; Atarashi, H.; Tanaka, K.; Jinnai, H. *Macromolecules* **2007**, *40*, 6940−6946.
(27) Yamauchi, K.; Takahashi, K.; Hasegawa, H.; Iatrou, H.; Hadjichristidis, N.; Kaneko, T.; Nishikawa, Y.; Jinnai, H.; Matsui, T.; Nishioka, H.; Shimizu, M.; Furukawa, H. *Macromolecules* **2003**, *36*, 6962−6966.
(28) Kaneko, T.; Suda, K.; Satoh, K.; Kamigaito, M.; Kato, T.; Ono, T.; Nakamura, E.; Nishi, T.; Jinnai, H. *Macromol. Symp.* **2006**, *242*, 80−86.
(29) Jinnai, H.; Kaneko, T.; Matsunaga, K.; Abetz, C.; Abetz, V. *Soft Matter* **2009**, *5*, 2042−2046.
(30) Hong, S.; Higuchi, T.; Sugimori, H.; Kaneko, T.; Abetz, V.; Takahara, A.; Jinnai, H. *Polym. J.* **2012**, *44* (6), 567−572.
(31) Luther, P. K.; Lawrence, M. C.; Crowther, R. A. *Ultramicroscopy* **1988**, *24*, 7−18.
(32) Crowther, R. A.; DeRosier, D. J.; Klug, A. *Proc. R. Soc. London* **1970**, *A 317*, 319−340.
(33) Winey, K. I.; Thomas, E. L.; Fetters, L. J. *Macromolecules* **1991**, *24*, 6182−6188.
(34) Winey, K.; Thomas, E. L.; Fetters, L. *J. Chem. Phys.* **1991**, *95*, 9367−9375.